Adsorption (2015) 21:205–215
DOI 10.1007/s10450-015-9663-y

Insights of water vapor sorption onto polymer based sorbents

Muhammad Sultan · Ibrahim I. El-Sharkawy · Takahiko Miyazaki · Bidyut B. Saha · Shigeru Koyama · Tomohiro Maruyama · Shinnosuke Maeda · Takashi Nakamura

Received: 23 October 2014 / Revised: 18 February 2015 / Accepted: 19 February 2015 / Published online: 1 March 2015

Abstract Two polymer based sorbents PS-I and PS-II are analyzed for water sorption applications. Adsorption/desorption isotherms of water vapor onto PS-I and PS-II have been experimentally measured using a magnetic suspension adsorption measurement unit for adsorber temperature ranges 20–80 °C and evaporator temperature ranges 2–73 °C. The equilibrium adsorption uptake of water vapors corresponding to saturation condition at 30 °C by PS-I and PS-II was found nearly 2 and 2.5 times higher than the conventional silica-gel, respectively. Adsorption data has been analyzed for various adsorption models which include Brunauer–Emmett–Teller (BET); Freundlich; Dubinin–Astakhov (D–A); Oswin; and Guggenheim–Anderson–de Boer (GAB) model. The GAB and BET model give the good fit for relative pressure range of 0.10–0.90 and 0.05–0.35, respectively. At all adsorption temperatures of both sorbents, the monolayer uptake by the GAB model is found higher than the BET model. Effect of adsorption potential on adsorption uptake is highlighted in relation with water vapor adsorption mechanism. The isosteric heat of water vapor adsorption is determined for both sorbents using Clausius–Clapeyron equation.

Keywords Adsorption isotherm · Water vapor · Polymer · Adsorption models

M. Sultan · B. B. Saha
Interdisciplinary Graduate School of Engineering Sciences, Kyushu University, 6-1 Kasuga-koen, Kasuga-shi, Fukuoka 816-8580, Japan

M. Sultan · I. I. El-Sharkawy · T. Miyazaki · B. B. Saha · S. Koyama
International Institute for Carbon-Neutral Energy Research (WPI-I2CNER), Kyushu University, 744 Motooka, Fukuoka 819-039, Japan

I. I. El-Sharkawy · T. Miyazaki (✉) · S. Koyama
Faculty of Engineering Sciences, Kyushu University, 6-1 Kasuga-koen, Kasuga-shi, Fukuoka 816-8580, Japan
e-mail: miyazaki.takahiko.735@m.kyushu-u.ac.jp

I. I. El-Sharkawy
Mechanical Power Engineering Department, Faculty of Engineering, Mansoura University, El-Mansoura, Egypt

T. Maruyama · S. Maeda · T. Nakamura
Green Technology Development Group, Global Technology Division, Calsonic Kansei Corporation, Sano-shi, Tochigi 327-0816, Japan

List of symbols

A	Polanyi's adsorption potential (kJ/kg)
A°, B°	Oswin model constants
C	BET and GAB model constant related to heat
E	Adsorption characteristic parameter (kJ/kg)
E (%)	Relative percentage deviation modulus
f_{GAB}, f_{BET}	Terms defined for linearization of GAB and BET models
GWP	Global warming potential
H_m	Monolayer heat of sorption (kJ/kg)
H_n	Multilayer heat of sorption (kJ/kg)
HVAC	Heating, ventilation and air-conditioning
K	Fitting parameter for GAB model
M	Equilibrium adsorption uptake (kg/kg)
M_m	Monolayer adsorption uptake (kg/kg)
M_o	Maximum adsorption capacity (kg/kg)
M_{mo}, q_m, C_o, K_o	GAB model adjustable constant for temperature effect
n	Fitting constant for D–A and Freundlich model (–)

ODP	Ozone depletion potential
P	Pressure (kPa)
P_o	Saturation pressure (kPa)
P/P_o	Relative pressure (–)
Q_{st}	Isosteric heat of sorption (kJ/kg)
R	Specific gas constant for water (kJ/kg-K)
T	Temperature (K)
T_{ads}	Adsorption/adsorber temperature (°C/K)
T_{eva}	Evaporator temperature (°C/K)
ΔH_c, ΔH_k	Functions related to water sorption heat (kJ/kg)
λ	Heat of condensation of water (kJ/kg)

1 Introduction

The thermally powered adsorption heat pump systems are receiving much attention as a replaceable eco-friendly technology for refrigeration and HVAC systems. The adsorption based systems ensures zero ODP and GWP, and can be operated on thermal heat source which gives opportunity to utilize low grade waste heat or solar thermal energy. Many adsorbent/refrigerant pairs have been experienced to establish an efficient and economic adsorption heat pump system which includes: (i) activated carbons with ethanol (El-Sharkawy et al. 2014), methanol (El-Sharkawy et al. 2009), ammonia (Tamainot-Telto and Critoph 1997), HCF410A (Askalany et al. 2014), HFO-1234ze(E) (Jribi et al. 2013), R134a (Saha et al. 2012) and n-butane (Saha et al. 2008); (ii) activated carbon fiber with ethanol (Saha et al. 2007); (iii) metal organic frameworks (MOFs) with water (Rezk et al. 2012), and ethanol (Rezk 2013); (iv) silica-gel with water (Saha et al. 1997), and ammonia (Sward 1999); (v) zeolite with CO_2 (Sward 1999), and water (Demir 2013); and many more.

Polymers are widely used in industries such as lubricant, rubber, membrane, hydrophobic adsorbent and medicine (Gun'ko et al. 2014), and therefore adsorption characteristics of polymers have been studied widely. Although the polymers and polymer based adsorbents have been utilized for many adsorption applications e.g. removal of chromium (Duranoğlu et al. 2010) and CO_2 capture/storage (Fan et al. 2014) but the use of polymer adsorbents in adsorption heat pump and cooling system is not so common as compared to carbon, silica-gel and zeolite. The sorption behavior in polymers is quite complex e.g. adsorption/absorption phenomena (Perret et al. 1972) and swelling/hysteresis phenomena (Smith 1947), and their intensity depends upon the nature of the polymer (like as polar/non-polar and mono-sulfonated/fully-sulfonated) and the employed conditions.

In the present study two kinds of polymer based sorbents are used for the water sorption analysis by utilizing gravimetric method. Adsorption data is fitted with various adsorption models and isosteric heat of adsorption is determined for each sorbent. The study focuses on the research parameters that need to address for establishing an adsorption heat pump system.

2 Materials and methods

2.1 Materials

Two kinds of novel polymer based sorbents namely PS-I and PS-II supplied by the Calsonic Kansei Corporation, Japan, are used for water sorption analysis. The particle size of the sorbents was determined by using 3D laser measuring microscope, OLS-4000 (LEXT). Laser microscope pictures for sorbent PS-I and PS-II are shown in Fig. 1a, b, respectively. The minimum, maximum and average particle sizes for both sorbents are determined which are listed in Table 1.

Bulk densities for PS-I, PS-II, and silica-gel (type RD) were measured by Micromeritics: GeoPyc 1360 Pycnometer provided by Micromeritics Instrument Corporation by applying pressure of 140, 280, 420 and 560 kPa. The particle diameter of RD type silica gel was varying from 1.0 to 1.81 mm whereas the particle size information of polymer sorbents is given in Table 1. The schematic diagram of the experimental unit is shown in Fig. 2a. At multiple consolidation conditions it measures the bulk volume by tapping/vibrating the sample within a graduated cylinder which is shown by component '2' in Fig. 2a. The displacement of plunger movement into the sample chamber is the actual measurement of the system which is further translated into bulk density. The plunger moves 2.6458E−4 cm along a screw with each motor pulse that drives the plunger. The calculated bulk densities for each sample are shown in Fig. 2b. Here it can be seen that the PS-II achieves nearly 1.5 and 1.16 times higher bulk density as compared to PS-I and silica-gel, respectively. Adsorbent density is important to ensure the promising system size for adsorption applications. Furthermore, the amount of adsorption uptake will also be increased if considered on volume basis (kg/m^3).

2.2 Description of the experimental setup

Sorption isotherms for PS-I and PS-II have been measured gravimetrically using magnetic suspension adsorption measurement unit (Rubotherm: MSB-VG-S2) provided by BEL Japan. Figure 3 shows the schematic diagram of the magnetic suspension adsorption measurement unit. The apparatus mainly include magnetics suspension adsorption

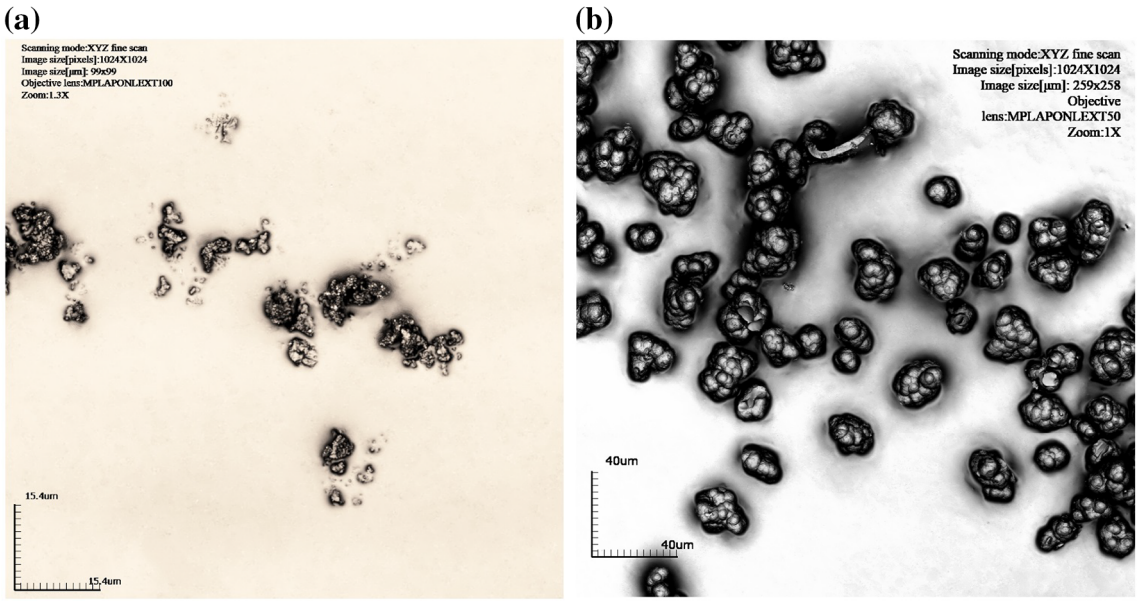

Fig. 1 Laser microscope image of few particles for: **a** PS-I; and **b** PS-II

Table 1 Minimum, maximum and average particle diameters of PS-I and PS-II

Diameter/sorbent (μm)	PS-I	PS-II
Minimum diameter	0.468	12.953
Maximum diameter	6.019	30.277
Average diameter	2.581	19.316

measurement unit; an evaporator with precise temperature control system; isothermal oil circulation baths to maintain adsorption/evaporation temperatures; isothermal air bath to ensure zero condensation within the system; a series of vacuum pumps including diaphragm, rotary and turbo-molecular types (with vacuum less than 3×10^{-5} Pa); and a PC along with data logger and software with automatic system control. The weight measurement repeatability of the magnetic balance is ±30 μg with the relative error of ±0.002 % of the reading. The system is employing nitrogen gas to control the valves whereas pressurized helium gas is used to ensure the leakage as well as to calculate the excluded volume of the adsorbed molecules which is required for buoyancy correction. As shown in Fig. 3, three kinds of absolute pressure gauges (1) 3500 kPa, Keller PAA-35XHTT-35; (2) 133.3 kPa, MKS 628B13TBE1B; and (3) 1.33 kPa, MKS 628B12TBE1B are used in parallel to measure the water vapor pressure with an accuracy of 0.15–0.25 %FS. The refrigerant's temperature is measured and controlled accurately by platinum resistance

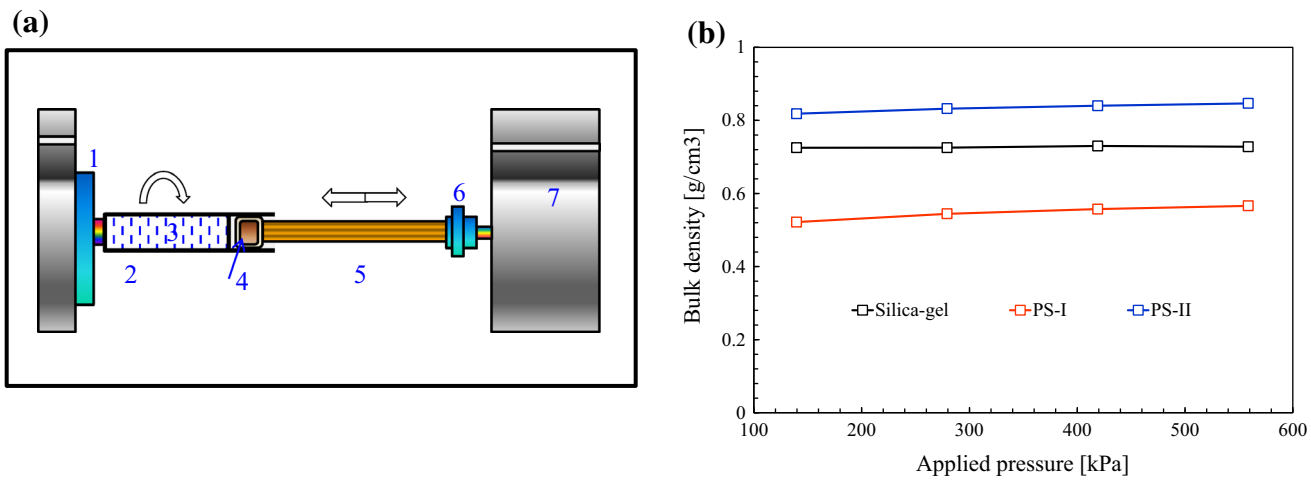

Fig. 2 **a** Schematic diagram of bulk density measurement unit. (1) left mandrel, (2) sample chamber, (3) sample, (4) plunger piston, (5) plunger, (6) right mandrel, and (7) pressure adjustment unit. **b** Bulk densities for PS-I, PS-II and silica-gel at different pressures

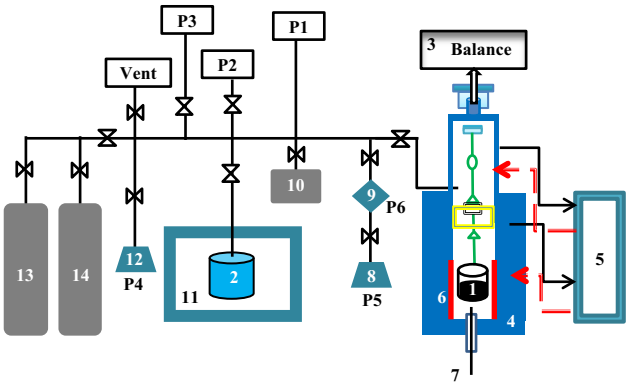

Fig. 3 Schematic diagram of the magnetic suspension adsorption measurement unit. (1) adsorbent, (2) refrigerant, (3) magnetic suspension balance, (4) oil circulation jacket, (5) isothermal oil bath, (6) high speed heater (regeneration), (7) thermocouples, (8) rotary pump, (9) turbo-molecular pump, (10) buffer, (11) isothermal oil bath, (12) diaphragm pump, (13) nitrogen gas, (14) helium gas, and (P1 to P6) pressure gauges

temperature element (100 Ω) together with pressure gauges which help in temperature adjustment to the corresponding to the vapor pressure. The system performs entire experiment automatically by following the instruction given through the software. The system provides flexibility in changing the recording interval (e.g. 1 s) as well as the equilibrium conditions (e.g. 10 μg for 60 s) of own choice which might need to change depending upon the nature of sorbents/refrigerant pair. The volume of the basket with the sample was measured using helium, which is a case for the measurement of excess adsorption (Talu 2013; Gumma and Talu 2010). Prior to each adsorption isotherm experiment, the helium bouncy measurements are performed at the isotherm temperature and pressure of 1.0 MPa. It is worth mentioning that the change in adsorbent volume due to swelling is marginal compared to the volume of the basket, and the bouncy is mainly affected by the volume of the basket, though the effect of adsorbent swelling isn't considered in this study.

The sorption amount was measured gravimetrically by the magnetic suspension balance without physical contact with the sample cell. The magnetic suspension unit consists of permanent magnet, sensor code and electronic control unit. To keep the sample in suspension, the electric signals are manipulated by the unit which is further translated into the sorption mass.

2.3 Experimental procedure

For each experiment nearly 90 mg of PS-I and PS-II were used for water sorption analysis. Using the multistep technique adsorption isotherms for each sample were obtained at 20, 30, 50, 70 and 80 °C whereas desorption isotherm were obtained at 30, 50 and 70 °C. For each adsorption temperature, the evaporator's temperature was varied from 2 °C to nearby adsorption temperature (which employs relative pressure $\cong 0.90$).

Initially samples were regenerated at 120 °C for 4 h under vacuum condition which approaches to 3×10^{-5} Pa for degassing the sample. Followed by regeneration, the sample was cooled to the set adsorption temperature and meanwhile the refrigerant temperature was maintained at first set point. Once the temperature on sample and refrigerant side became steady the valves were opened for adsorption. The system recorded the adsorption of water vapors for each second until the equilibrium condition arises and after that refrigerant temperature was increased to the next set point. Similarly water vapor adsorption was recorded for all the set refrigerant temperatures. The same procedure was followed for desorption isotherms by decreasing the refrigerant temperature.

3 Data analysis

3.1 Modelling of sorption isotherms

The adsorption data is analyzed for various adsorption models which include; (i) Brunauer–Emmett–Teller (BET) (Brunauer et al. 1938); (ii) Freundlich (1926); (iii) Dubinin–Astakhov (D–A) (Dubinin 1967; Dubinin and Astakhov 1971); (iv) Oswin (1946); and (v) Guggenheim (1966), Anderson (1946), De Boer (1953) (GAB). The BET theory is based on simple two parametric model of multilayer sorption which represents the development of monolayer Langmuir sorption model. The BET theory well describes the mono/multilayer gas adsorption on nonporous adsorbents and also considered for water sorption analysis on polymers (Toribio et al. 2004). Two parameters based an empirical expression of Freundlich model was recognized as early as 1926 by Freundlich (1926) which was later derived theoretically using various approaches (Hayward and Trapnell 1964; Sips 1950, 1948). This kind of isotherms are observed for many heterogeneous surfaces including activated carbon, silica, clays, metals, and polymers (Umpleby II et al. 2001). Oswin (1946) developed an empirical sorption isotherm model which has been found a good fit water sorption model for various foods products as well as for pectin, a bio polymer (Basu et al. 2013). The D–A equation, a generalized version of the Dubinin–Radushkevich (D–R) equation (where parameter $n = 2$) is based on micropore volume filling theory which is related to Polanyi's adsorption potential theory (Hutson and Yang 1997). The theory is widely used for micropore adsorption on carbons (El-Sharkawy et al. 2014, 2009) and also considered for carbonized polymers (Rand 1976). The corresponding mathematical

expression for adsorption models and their linear forms are given in Table 2. The parameters of each model are identified in the nomenclature. Linear technique is used to determine the model parameters and goodness of the fit by minimizing the mean relative percentage deviation modulus, E (%) which is defined as:

$$E\ (\%\ ) = \frac{100}{N}\sum_{i=1}^{N}\left[\frac{\left|M_{exp} - M_{cal}\right|}{M_{exp}}\right] \quad (1)$$

Where N is the number of experimental points, M_{exp} is experimental and M_{cal} is calculated adsorption uptakes (kg/kg).

The GAB model which is represented by Eq. (2) is widely used for moisture sorption analysis of food products (Akanbi et al. 2006; Menkov and Dinkov 1999). Apart from the food product the model is also used for different kind of adsorbents e.g. bentonite (Mihoubi and Bellagi 2006), nanoparticles (Ribeyre et al. 2014) and lignite (Pakowski et al. 2011) etc. The GAB model is an improvement of the BET theory and shares two of its constants (i) 'M_m' the monolayer capacity, and (ii) 'C' the analogous formulation of the BET constant C_{BET}. The GAB models provide its versatility with a third constant 'K' and can be interconnected with the BET constants as given in Eq. (3–4). If this third constant 'K' is equal to unity, the GAB equation is thus reduced to BET equation.

$$M = \frac{M_m CK(P/P_o)}{[(1 - K(P/P_o)][(1 - K(P/P_o) + CK(P/P_o)]} \quad (2)$$

$$C_{BET} = C_{GAB}K \quad (3)$$

$$C_{BET} = C_{GAB} \quad \text{when } K = 1 \quad (4)$$

All three constants of GAB model (M_m, C, K) have the physical meaning and can be written as functions of adsorption temperature:

$$M_m = M_{mo}\exp\left(\frac{q_m}{RT_{ads}}\right) \quad (5)$$

$$C = C_o \exp\left(\frac{\Delta H_c}{RT_{ads}}\right) \quad (6)$$

$$K = K_o \exp\left(\frac{\Delta H_k}{RT_{ads}}\right) \quad (7)$$

Where T_{ads} is absolute temperature (K); R is specific gas constant for water (kJ/kg-K); M_{mo}, q_m, C_o, and K_o are the adjustable constants for the temperature effect. ΔH_c and ΔH_k are functions of heat of water sorption which can be written as:

$$\Delta H_c = H_m - H_n \quad (8)$$

$$\Delta H_k = \lambda - H_n \quad (9)$$

The λ represents the heat of condensation of water (kJ/kg) whereas H_m and H_n are the heat of water sorption of monolayer and multilayer (kJ/kg), respectively.

Direct and indirect techniques can be employed to estimate the constants of GAB model from the experimental data by minimizing the mean relative percentage deviation modulus, E (%). In the direct technique the six constants of GAB model (M_{mo}, q_m, C_o, K_o, ΔH_c, ΔH_k) are calculated by inserting the Eq. (5–7) in Eq. (2). However, in the indirect technique the three constants (M_m, C, K) are estimated at first on each temperature and then the six constants (M_{mo}, q_m, C_o, K_o, ΔH_c, ΔH_k) are calculated by using the three constants. The reliability of indirect technique depends on the M_m, C and K regions that are obtained from the first estimation. The indirect technique is not recommended because the basic three constants of the GAB equation are interconnected with each other (Maroulis et al. 1988). Hence in the present study the constants of the GAB model are estimated by the fit of the equation using the direct technique.

3.2 Isosteric heat of sorption

The isosteric heat of sorption or enthalpy of sorption (Q_{st}) is the difference between the activation energy of adsorption and desorption, and it represents the strength of adsorbent-refrigerant interaction (Szekely et al. 1976). It is difficult to measure the isosteric heat of adsorption experimentally. However, using the GAB adsorption model with calculated fitting parameters, the isosteric heat of adsorption (Q_{st}) can be determined by the Clausius–Clapeyron relationship for certain uptake:

Table 2 Adsorption isotherm models used for fitting of the experimental data

Model	Mathematical expression	Linear form	No. of parameters
BET	$M = \frac{M_m C_{BET}(P/P_o)}{[(1-(P/P_o)][(1-(P/P_o)+C_{BET}(P/P_o)]}$	$f_{BET} = \frac{(P/P_o)}{M(1-(P/P_o))} = \frac{1}{M_m C_{BET}} + \left(\frac{C_{BET}-1}{M_m C_{BET}}\right)(P/P_o)$	2
D–A	$M = M_o \exp\left[-\left(\frac{A}{E}\right)^n\right]; A = R\ T_{ads} \ln\left(\frac{P_o}{P}\right)$	$\ln(M) = \ln(M_o) - \left(\frac{1}{E}\right)^n \left(RT_{ads}\ln\left(\frac{P_o}{P}\right)\right)^n$	3
Oswin	$M = A^o\left[\frac{(P/P_o)}{1-(P/P_o)}\right]^{B^o}$	$\ln M = \ln A^o + B^o \ln\left(\frac{(P/P_o)}{1-(P/P_o)}\right)$	2
GAB	$M = \frac{M_m CK(P/P_o)}{[(1-K(P/P_o)][(1-K(P/P_o)+CK(P/P_o)]}$	$f_{GAB} = \frac{(P/P_o)}{M(1-K(P/P_o))} = \frac{1}{M_m CK} + \left(\frac{C-1}{M_m C}\right)(P/P_o)$	3

$$\frac{Q_{st}}{R} = -\left[\frac{\partial \ln P}{\partial(1/T_{ads})}\right]_M \tag{10}$$

Where Q_{st} is the isosteric heat of sorption (kJ/kg) and R is specific gas constant for water (kJ/kg-K). Q_{st} can be determined by the slope obtained from the linear plot between ln(P) and $(1/T_{ads})$. Using GAB equation the ln(P) can be calculated by the following relationship:

$$\ln(P) = \ln(P_o) + \ln\left(\frac{[(M_mC/M) + 2 - C] - \sqrt{[(M_mC/M) + 2 - C]^2 - 4(1 - C)}}{2K(1 - C)}\right) \tag{11}$$

4 Results and discussion

Water vapor adsorption/desorption isotherms by two polymer sorbents PS-I and PS-II are measured gravimetrically at adsorption temperatures between 20 and 80 °C. A little hysteresis is observed in adsorption data, though the effect is minimized at adsorption temperature more than 50 °C. Figure 4a, b show the hysteresis loop on water vapor adsorption–desorption isotherm at 70 °C for PS-I and PS-II, respectively. It can be seen that the both polymer sorbents enable minor hysteresis at higher temperature which is favorable for the regeneration process of an adsorption heat pump system.

Water vapor adsorption isotherms at 20, 30, 50, 70 and 80 °C for PS-I and PS-II are shown in Fig. 5a, b, respectively. The equilibrium water vapor uptake corresponding to saturation condition at 30 °C by conventional silica-gel (RD type) is almost 0.40 kg/kg (Sultan et al. 2014). However, at the same conditions, polymer sorbents PS-I and PS-II are enabling nearly 2 and 2.5 times higher adsorption amount as compared to silica-gel, respectively. Figure 5 shows that the both samples enable relatively linear trend of adsorption isotherms at lower adsorption temperatures whereas sigmoid shaped isotherms are obtained on higher adsorption temperatures. The fact can be more visible if the adsorption data (on Fig. 5) is plotted against relative pressure. This kind of phenomena is promising for designing an open-cycle and/or close-cycle adsorption heat pump systems.

The adsorption data is analyzed for well-known adsorption models that include: BET, Freundlich, D–A, Oswin, and GAB. The constants of the GAB model are estimated by the fit of the equation using the direct technique as explained under Sect. 3.1. The fitting parameters for BET, Freundlich, D–A and Oswin adsorption models are calculated through the slope and intercept of the linear plots of the corresponding equations (see Table 2). However, the Freundlich model and its results are not incorporated in the article because of the maximum fitting error (E = 2–18 %). The fitting results of each adsorption model for PS-I and PS-II are given in

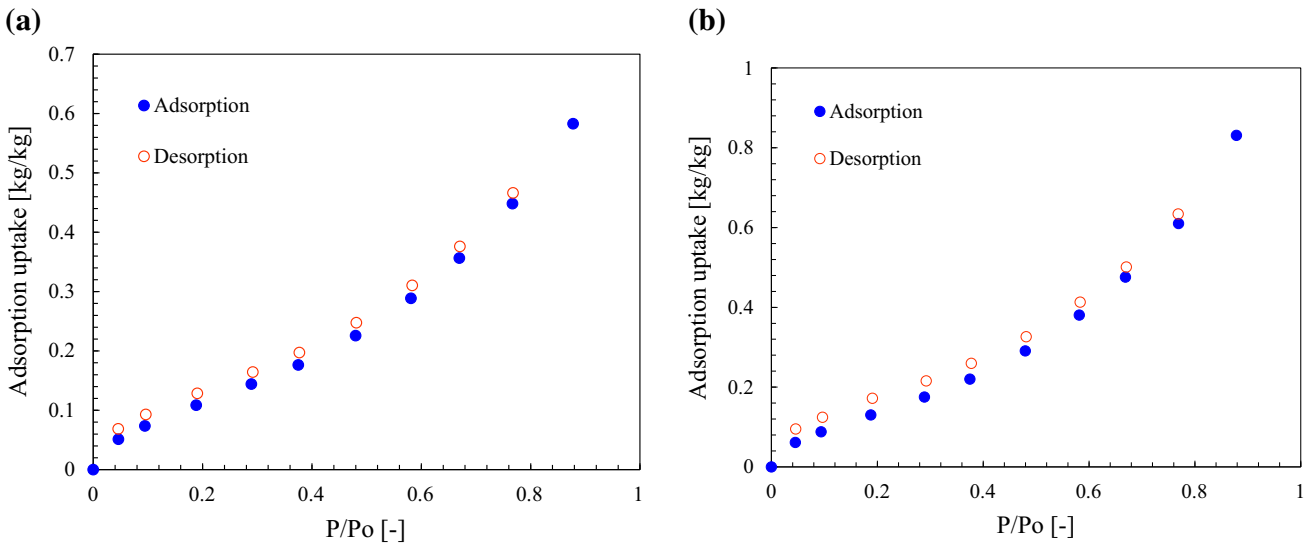

Fig. 4 Hysteresis loop on water vapor adsorption–desorption isotherm at 70 °C for: **a** PS-I; and **b** PS-II

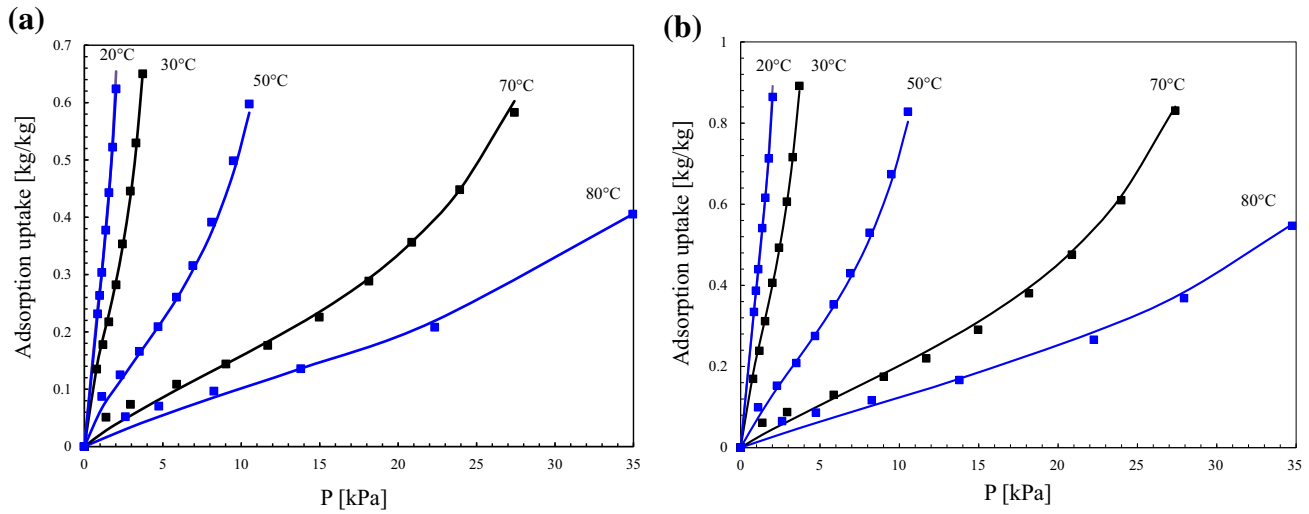

Fig. 5 Water vapor adsorption isotherms at 20, 30, 50, 70 and 80 °C for: **a** PS-I; and **b** PS-II. Symbol represents the experiment whereas lines represent the GAB model

Table 3 Estimated parameters of adsorption models for PS-I and PS-II

Adsorption model	Fitting range (P/P_o)	Estimated parameters	PS-I					PS-II				
			20 °C	30 °C	50 °C	70 °C	80 °C	20 °C	30 °C	50 °C	70 °C	80 °C
BET model	0.05–0.35	M_m (kg/kg)	–	0.168	0.149	0.124	0.115	–	0.266	0.202	0.155	0.14
		C_{BET} (–)	–	8.008	10.07	11.86	11.76	–	4.752	7.74	10.85	12.11
		R^2	–	0.999	0.998	0.996	0.996	–	0.996	0.989	0.992	0.991
		E (%)	–	0.41	1.30	3.14	2.77	–	0.89	3.31	4.40	3.83
D–A model	0.05–0.90	M_o (kg/kg)	1.20					1.76				
		E (kJ/kg)	47.37					41.84				
		n (–)	0.50					0.50				
		R^2	0.992					0.983				
		E (%)	5.10					7.66				
Oswin model	0.05–0.90	A^o	0.312	0.285	0.269	0.234	0.226	0.451	0.392	0.353	0.303	0.294
		B^o	0.407	0.478	0.50	0.51	0.53	0.383	0.491	0.536	0.542	0.556
		R^2	0.979	0.987	0.997	0.997	0.998	0.979	0.978	0.994	0.996	0.995
		E (%)	4.39	4.98	2.74	3.56	2.56	4.07	6.86	4.13	4.57	4.65
GAB model	0.10–0.90	M_{mo} (kg/kg)	0.058					0.0418				
		C_o (–)	0.256					0.143				
		K_o (–)	1.155					1.7944				
		q_m (kJ/kg)	202.378					308.528				
		ΔH_c (kJ/kg)	433.408					489.02				
		ΔH_k (kJ/kg)	−60.48					−129.89				
		R^2	0.995					0.996				
		E (%)	2.95					3.14				

Table 3 which clarifies the distinction of GAB model over the others. It can be seen from Fig. 5a, b that the GAB model gives the good fit for all adsorption temperatures of PS-I and PS-II, respectively. For the relative pressure range of 0.10–0.90, the mean relative percentage deviation modulus (E) is found 2.95 and 3.14 % for PS-I and PS-II, respectively.

The both polymer sorbents presents sigmoid shaped adsorption isotherms having concave shape at the initial range of P/P_o followed by the convex shape as shown in

Figs. 4 and 5. Smith (1947) described this reason by considering two principal classes of sorbed water; firstly that which is normally condensed within the polymer and it is the function of relative pressure (i.e. responsible to convex shape); and secondly by which the water is bound on the inner/outer surface of the polymer by forces in excess of the normal forces (i.e. responsible to concave shape). The adsorption amount by the concave region gets its maximum value at P/P_o well shorter than saturation especially for polar adsorbents-refrigerants, and even for the non-polar adsorbate (nitrogen) it comes at $P/P_o = 0.10$ (Brunauer et al. 1938). The GAB model could not represent these extraordinary forces responsible to formation of concave region and hence the adsorption uptake at $P/P_o < 0.10$ is underestimated by the model as shown in Fig. 5.

To have the better fit of the data at lower relative pressure the BET model is employed due to its consistency at lower P/P_o. The BET model gives good fit for all adsorption temperatures of PS-I and PS-II as shown in Fig. 6.

For the both samples the monolayer uptake (M_m) determined by the GAB model is found higher than the BET model and the value decreases with the increase in adsorption temperature as shown in Fig. 7. Goula et al. (2008) also reported the similar behavior of monolayer uptake by BET and GAB models. In polymers, the water molecules condense in multiple layers on the first layer. Each molecule in the top most layer replaces an equivalent molecule in the first layer which is prevented by its over burden from evaporating (Smith 1947). This means the first layer adsorption amount is the function of P/P_o and it completes at saturation. As the BET model is fitted at relatively lower P/P_o range (i.e. 0.05–0.35) as compared to GAB model (i.e. 0.10–0.90) so the numeric values of monolayer uptakes by the BET model were found lower as compared to the GAB model.

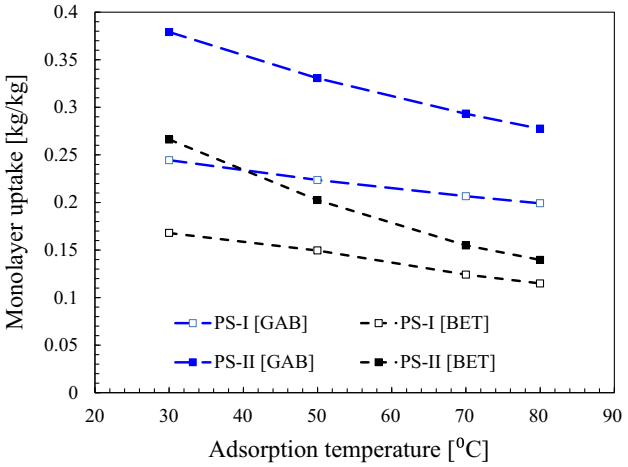

Fig. 7 Monolayer uptake comparison by BET and GAB model for PS-I and PS-II

Using experimental data the Polanyi's adsorption potential for PS-I and PS-II is calculated by the following equation.

$$A = R\ T_{ads} \ln\left(\frac{1}{P/P_o}\right) \tag{12}$$

The adsorption amount is decreasing with the increase in Polanyi's adsorption potential for PS-I and PS-II with the similar trend as shown in Fig. 8. It means that the PS-I and PS-II probably follow the same water vapor adsorption mechanism. Furthermore most of the uptake occurs at lower adsorption potential which is the region of higher relative pressure hence less molar work is required for adsorption at higher relative pressure. To avoid the condensation, the experimental data of water vapor adsorption on both samples covered the maximum relative pressure of nearly 0.88 only. However, Fig. 8 shows that there is still an exponentially increasing trend of

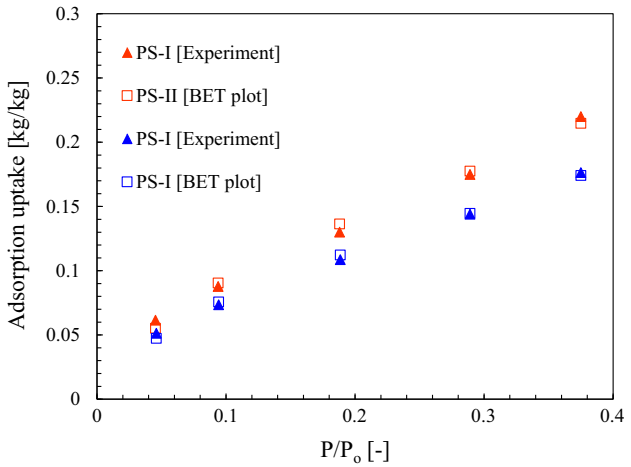

Fig. 6 Comparison of BET plot with experimental data for PS-I and PS-II at 70 °C

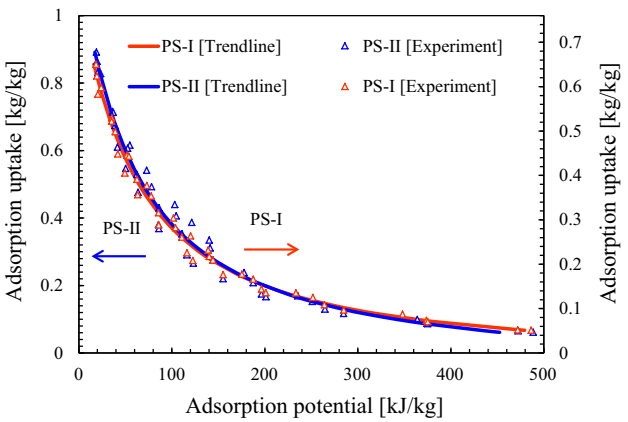

Fig. 8 Comparison of Polanyi's adsorption potential with adsorption uptake for PS-I and PS-II

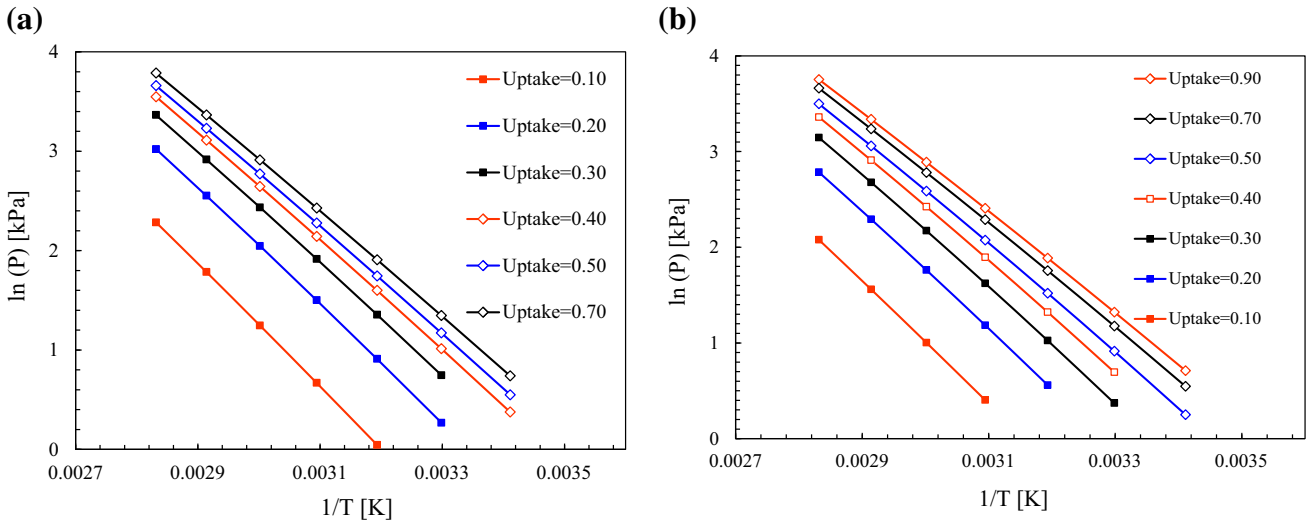

Fig. 9 Linear plot of ln(P) versus $1/T_{ads}$ at different water vapor uptakes for: **a** PS-I; and **b** PS-II

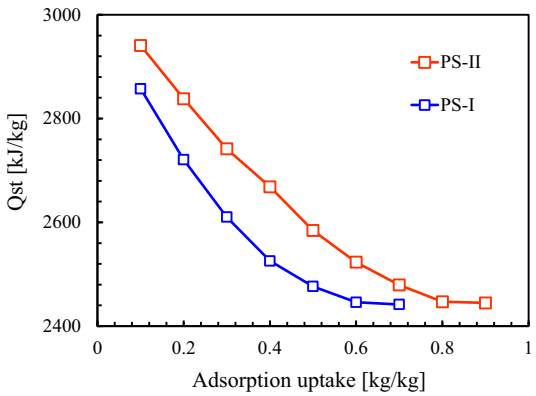

Fig. 10 Plot of isosteric heat of water vapors adsorption versus adsorption uptake for PS-I and PS-II

adsorption uptake for PS-I and PS-II near to the zero adsorption potential (approaches to saturation pressure) due to utilization of the least molar work. This way of adsorption can be effective for adsorption air-conditioning system by utilizing pre-cooling below the dew point. As the polymers usually undergo limited or unlimited swelling which increase the number of sportive points exposed within the structure. So the sorption amount is not only dependent to the P/P_o but also effective sorption surface after swelling (Smith 1947). Figure 8 also reveals that the PS-I and PS-II probably follow the similar kind of swelling phenomena which is independent from the total sorption amount.

The isosteric heat of water vapor adsorption (Q_{st}) is calculated using the Clausius–Clapeyron relationship by means of equilibrium adsorption data produced by GAB model. The slope of the linear plot between ln(P) and $1/T_{ads}$ will yield the amount equal to $-Q_{st}/R$ as shown in Fig. 9a, b. These plots are useful for evaluation of close-cycle adsorption heat pump system. The amount of Q_{st} decreases with the increase in adsorption uptake as shown in Fig. 10. The average isosteric heat of adsorption for PS-I and PS-II is found 2665 and 2708 kJ/kg, respectively. The isosteric heat of adsorption for both samples does not extremely vary as compared to conventional silica-gel which will ensure promising results for adsorption heat pump system.

5 Conclusions

Adsorption/desorption isotherms of water vapor onto two polymer based sorbents PS-I and PS-II have been experimentally measured using a magnetic suspension adsorption measurement unit at adsorption temperature ranges 20–80 °C and evaporator temperature ranges 2–73 °C. The equilibrium adsorption uptake corresponding to saturation condition at 30 °C by PS-I and PS-II is found nearly 2 and 2.5 times higher than the conventional silica-gel, respectively. The experimental data is analyzed by BET, Freundlich, D–A, Oswin and GAB adsorption models. The GAB model gives the good fit under all adsorption temperatures for the relative pressure range of 0.10–0.90. The mean relative percentage deviation modulus is found 2.95 and 3.14 % for PS-I and PS-II, respectively. Moreover, the BET model gives the good fit for the lower relative pressure range of 0.05–0.35. At all adsorption temperatures of both sorbents, the monolayer uptake by the GAB model is found higher than the BET model. A similar effect of adsorption potential on adsorption uptake is found by the both sorbents which is independent to the total

adsorption amount. This means both sorbents enable same adsorption mechanism and probably follow the similar kind of swelling phenomena. The isosteric heat of water vapor adsorption is determined by Clausius–Clapeyron equation and GAB model. The average isosteric heat of adsorption is found 2665 and 2708 kJ/kg for PS-I and PS-II, respectively.

Acknowledgments This work was supported by TherMAT Project, Japan Ministry of Economy, Trade and Industry (METI).

References

Akanbi, C.T., Adeyemi, R.S., Ojo, A.: Drying characteristics and sorption isotherm of tomato slices. J. Food Eng. **73**, 157–163 (2006)

Anderson, R.B.: Modifications of the Brunauer, Emmett and Teller Equation 1. J. Am. Chem. Soc. **68**, 686–691 (1946)

Askalany, A.A., Saha, B.B., Ismail, I.M.: Adsorption isotherms and kinetics of HFC410A onto activated carbons. Appl. Therm. Eng. **72**, 237–243 (2014)

Basu, S., Shivhare, U.S., Muley, S.: Moisture adsorption isotherms and glass transition temperature of pectin. J. Food Sci. Technol. **50**, 585–589 (2013)

De Boer, J.H.: The Dynamical Character of Adsorption. Clarendon, Oxford (1953)

Brunauer, S., Emmett, P.H., Teller, E.: Adsorption of gases in multimolecular layers. J. Am. Chem. Soc. **60**, 309–319 (1938)

Demir, H.: Development of microwave assisted zeolite–water adsorption heat pump. Int. J. Refrig **36**, 2289–2296 (2013)

Dubinin, M.M.: Adsorption in micropores. J. Colloid Interface Sci. **23**, 487–499 (1967)

Dubinin, M.M., Astakhov, V.A.: Development of the concepts of volume filling of micropores in the adsorption of gases and vapors by microporous adsorbents. Bull. Acad. Sci. USSR Div. Chem. Sci. **20**, 3–7 (1971)

Duranoğlu, D., Trochimczuk, A.W., Beker, Ü.: A comparison study of peach stone and acrylonitrile-divinylbenzene copolymer based activated carbons as chromium(VI) sorbents. Chem. Eng. J. **165**, 56–63 (2010)

El-Sharkawy, I.I., Hassan, M., Saha, B.B., Koyama, S., Nasr, M.M.: Study on adsorption of methanol onto carbon based adsorbents. Int. J. Refrig **32**, 1579–1586 (2009)

El-Sharkawy, I.I., Uddin, K., Miyazaki, T., Saha, B.B., Koyama, S., Miyawaki, J., Yoon, S.-H.: Adsorption of ethanol onto parent and surface treated activated carbon powders. Int. J. Heat Mass Transf. **73**, 445–455 (2014)

Fan, Y., Lively, R.P., Labreche, Y., Rezaei, F., Koros, W.J., Jones, C.W.: Evaluation of CO2 adsorption dynamics of polymer/silica supported poly(ethylenimine) hollow fiber sorbents in rapid temperature swing adsorption. Int. J. Greenh. Gas Control. **21**, 61–71 (2014)

Freundlich, H.: Colloid and Capillary Chemistry. Methuen, London (1926)

Goula, A.M., Karapantsios, T.D., Achilias, D.S., Adamopoulos, K.G.: Water sorption isotherms and glass transition temperature of spray dried tomato pulp. J. Food Eng. **85**, 73–83 (2008)

Guggenheim, E.A.: Applications of Statistical Mechanics. Clarendon, Oxford (1966)

Gumma, S., Talu, O.: Net adsorption: a thermodynamic framework for supercritical gas adsorption and storage in porous solids. Langmuir **26**, 17013–17023 (2010)

Gun'ko, V.M., Turov, V.V., Turova, A.A., Krupska, T.V., Pissis, P., Leboda, R., Skubiszewska-Zięba, J.: Interactions of poly(dimethylsiloxane) with nanosilica and silica gel upon cooling–heating. J. Colloid Interface Sci. 426, 48–55 (2014)

Hayward, D.O., Trapnell, B.M.W.: Chemisorption. Butterworths, London (1964)

Hutson, N.D., Yang, R.T.: Theoretical basis for the Dubinin-Radushkevitch (D-R) adsorption isotherm equation. Adsorption. **3**, 189–195 (1997)

Jribi, S., Saha, B.B., Koyama, S., Chakraborty, A., Ng, K.C.: Study on activated carbon/HFO-1234ze(E) based adsorption cooling cycle. Appl. Therm. Eng. **50**, 1570–1575 (2013)

Maroulis, Z.B., Tsami, E., Marinos-Kouris, D., Saravacos, G.D.: Application of the GAB model to the moisture sorption isotherms for dried fruits. J. Food Eng. **7**, 63–78 (1988)

Menkov, N.D., Dinkov, K.T.: Moisture sorption isotherms of tobacco seeds at three temperatures. J. Agric. Eng. Res. **74**, 261–266 (1999)

Mihoubi, D., Bellagi, A.: Thermodynamic analysis of sorption isotherms of bentonite. J. Chem. Thermodyn. **38**, 1105–1110 (2006)

Oswin, C.R.: The kinetics of package life. III. The isotherm. J. Soc Chem. Ind. **65**, 419–421 (1946)

Pakowski, Z., Adamski, R., Kokocińska, M., Kwapisz, S.: Generalized desorption equilibrium equation of lignite in a wide temperature and moisture content range. Fuel **90**, 3330–3335 (2011)

Perret, E.A., Stoeckli, H.F., Jeanneret, C.: Surface chemistry of polymers, adsorption and absorption of gases by polyvinylchloride. Helv. Chim. Acta **55**, 1987–1991 (1972)

Rand, B.: On the empirical nature of the Dubinin—Radushkevich equation of adsorption. J. Colloid Interface Sci. **56**, 337–346 (1976)

Rezk, A., Al-Dadah, R., Mahmoud, S., Elsayed, A.: Characterisation of metal organic frameworks for adsorption cooling. Int. J. Heat Mass Transf. **55**, 7366–7374 (2012)

Rezk, A., AL-Dadah, R., Mahmoud, S., Elsayed, A.: Investigation of ethanol/metal organic frameworks for low temperature adsorption cooling applications. Appl. Energy **112**, 1025–1031 (2013)

Ribeyre, Q., Grévillot, G., Charvet, A., Vallières, C., Thomas, D.: Modelling of water adsorption–condensation isotherms on beds of nanoparticles. Chem. Eng. Sci. **113**, 1–10 (2014)

Saha, B.B., Akisawa, A., Kashiwagi, T.: Silica gel water advanced adsorption refrigeration cycle. Energy. **22**, 437–447 (1997)

Saha, B.B., Chakraborty, A., Koyama, S., Yoon, S.-H., Mochida, I., Kumja, M., Yap, C., Ng, K.C.: Isotherms and thermodynamics for the adsorption of n-butane on pitch based activated carbon. Int. J. Heat Mass Transf. **51**, 1582–1589 (2008)

Saha, B.B., El-Sharkawy, I.I., Chakraborty, A., Koyama, S.: Study on an activated carbon fiber–ethanol adsorption chiller: part II—performance evaluation. Int. J. Refrig **30**, 96–102 (2007)

Saha, B.B., El-Sharkawy, I.I., Thorpe, R., Critoph, R.E.: Accurate adsorption isotherms of R134a onto activated carbons for cooling and freezing applications. Int. J. Refrig **35**, 499–505 (2012)

Sips, R.: On the structure of a catalyst surface. J. Chem. Phys. **16**, 490–495 (1948)

Sips, R.: On the structure of a catalyst surface II. J. Chem. Phys. **18**, 1024–1026 (1950)

Smith, S.E.: The sorption of water vapor by high polymers. J. Am. Chem. Soc. **69**, 646–651 (1947)

Sultan, M., El-Sharkawy, I.I., Miyazaki, T., Saha, B.B., Koyama, S.: Experimental study on carbon based adsorbents for greenhouse dehumidification. Evergreen. 01, 5–11 (2014)

Sward, B.K., LeVan, M.D.: Examination of the performance of a compression-driven adsorption cooling cycle. Appl. Therm. Eng. **19**, 1–20 (1999)

Szekely, J., Evans, J.W., Sohn, H.Y.: Gas-Solid Reactions. Academic Press, New York (1976)

Talu, O.: Net adsorption of gas/vapor mixtures in microporous solids. J. Phys. Chem. C **117**, 13059–13071 (2013)

Tamainot-Telto, Z., Critoph, R.E.: Adsorption refrigerator using monolithic carbon-ammonia pair. Int. J. Refrig **20**, 146–155 (1997)

Toribio, F., Bellat, J.P., Nguyen, P.H., Dupont, M.: Adsorption of water vapor by poly(styrenesulfonic acid), sodium salt: isothermal and isobaric adsorption equilibria. J. Colloid Interface Sci. **280**, 315–321 (2004)

Umpleby II, R.J., Baxter, S.C., Bode, M., Berch Jr, J.K., Shah, R.N., Shimizu, K.D.: Application of the Freundlich adsorption isotherm in the characterization of molecularly imprinted polymers. Anal. Chim. Acta **435**, 35–42 (2001)